**Proceedings of the ASME 2010 International Design Engineering Technical Conferences & Computers and Information in Engineering Conference**
**IDETC/CIE 2010**
**August 15-18, 2010, Montreal, Quebec, Canada**

# DETC2010-28962

## DEVELOPMENT OF A FIVE-BAR PARALLEL ROBOT WITH LARGE WORKSPACE

**Lucas Campos, Francis Bourbonnais, Ilian A. Bonev, and Pascal Bigras**
École de technologie supérieure (ÉTS), Montreal, QC, Canada

### ABSTRACT

Five-bar planar parallel robots for pick and place operations are always designed so that their singularity loci are significantly reduced. In these robots, the length of the proximal links is different from the length of the distal links. As a consequence, the workspace of the robot is significantly limited, since there are holes in it. In contrast, we propose a design in which all four links have equal lengths. Since such a design leads to more parallel singularities, a strategy for avoiding them by switching working modes is proposed. As a result, the usable workspace of the robot is significantly increased. The idea has been implemented on an industrial-grade prototype and the latter is described in detail.

### 1. INTRODUCTION

It is well known that the workspace of a parallel robot is generally smaller than that of a similar-sized serial robot and is often segmented by singularities. There is a need in industry for robots capable of doing optimal use of the limited workspace that characterizes parallel robots.

Loosely speaking, singularities are configurations where the inherent rigidity of a parallel robot suddenly changes. Most parallel robots have two types of singularities. *Type* 1 *singularities* (also called *serial singularities*) are configurations in which the end-effector loses one or several degrees of freedom (DOFs). These basically correspond to the workspace boundary of a parallel robot. *Type* 2 *singularities* (also called *parallel singularities*) are more complex configurations where the actuators cannot resist a force and/or moment applied to the end-effector. They are inside the workspace, splitting it into various singularity-free segments.

The conventional approach used in industry is to compromise the workspace-to-footprint ratio and optimize the robot's design so as to remove Type 2 singularities [1]. Another typical approach is to leave Type 2 singularities inside the workspace and navigate within a single singularity-free region [2,3]. However, even if this region is maximized [4], it remains smaller than the complete workspace.

A more direct approach to making better use of the workspace consists in reducing Type 2 singularities of a parallel robot through the use of redundant actuation [5]. However, this brings greater complexity to the control problem and additional cost.

If precise continuous motion is required, such as in machining, all types of singularities must be avoided using one of the above approaches. However, if only discrete poses of the end-effector need to be accurate, such as in material handling, the path between two poses need not necessarily be precise and may therefore involve singularities. The question is how to enable a parallel robot to navigate through singularities in order to make optimal use of its workspace.

The most direct approach is to confront Type 2 singularities using external force, such as inertia [6,7]. This looks like the best approach with respect to workspace optimization, but the fact is that precision is lost in areas close to Type 2 singularities. So, basically, the usable workspace becomes highly disconnected.

Parallel robots that have several working modes (solutions to the inverse kinematics) generally have different Type 2 singularities for the different working modes [8,9]. Therefore, it is possible to reach any point from the complete workspace (or from a large part of it) without compromising accuracy and inherent rigidity, simply by switching working modes. Changing working modes implies passing through Type 1 singularities only, which is easily achieved using active-joint control [7].

This paper discusses the development of a planar parallel robot built in order to investigate the effectiveness of the approach of switching working modes. This robot is similar to the industrial "double-SCARA" robot offered by Mitsubishi Electric (a 2-DOF planar parallel robot with revolute actuators, also known as "five-bar") for rapid material handling, and it is dubbed DexTAR (Dexterous Twin-Arm Robot).

The paper recalls the theoretical results presented in [10] and goes a step further, substantiating the claims on a real prototype. Section 2 will describe the kinematics of our planar parallel robot and discuss its practical optimization. In Sections 3 and 4, we will describe the mechanical design of

our robot and its real attainable workspace, respectively. Section 5 will briefly outline the trajectory planning problem. Conclusions are presented in the last section.

## 2. OPTIMUM DESIGN OF THE FIVE-BAR PARALLEL ROBOT

In [7], the authors present a work very similar to ours, but on a 2-DOF PRRRP planar parallel robot. (In this paper, P and R stand for prismatic and revolute joints, respectively, and an underline means that the joint is actuated). In addition, the authors force their parallel robot to cross Type 2 singularities. Without doing so, and only switching working modes, they obtain no workspace gain at all. In our paper, we will not only show that a significant workspace gain is possible without crossing Type 2 singularities, but we will also address the more practical RRRRR robot (revolute actuators being much cheaper than prismatic actuators), whose schematics is shown in Fig. 1 and for which a Java applet is available at http://www.parallemic.org/Java/FiveBar.html.

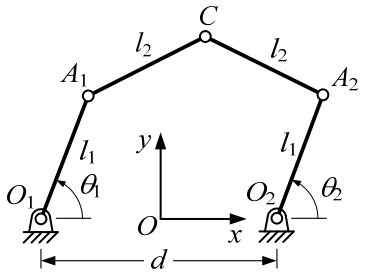


**Fig. 1.** Schematics of a 2-DOF RRRRR planar parallel robot.

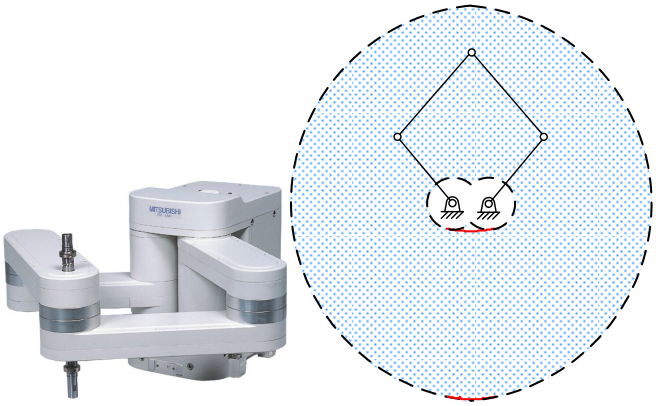

(a) (b)

**Fig. 2.** (a) RP-5AH industrial robot (courtesy of Mitsubishi Electric) and (b) its optimized theoretical singularity-free workspace (the hatched area) as part of its complete workspace.

A RRRRR planar parallel robot has already been commercialized by Mitsubishi Electric (Fig. 2). Their RP-series industrial robot, offered in three sizes, is basically a double-SCARA robot offering better cycle times and higher precision than conventional SCARA robots.

Figure 2a shows the largest model, RP-5AH, whose dimensions are $d = 85$ mm, $l_1 = 200$ mm and $l_2 = 260$ mm (where $d$, $l_1$ and $l_2$ are as defined in Fig. 1). Figure 2b shows the robot's theoretical workspace (excluding mechanical interferences), where the workspace boundary (the Type 1 singularity loci) is drawn in black dashed line and its Type 2 singularity loci are drawn in solid red line. The workspace is well optimized, as Type 2 singularities are nearly absent. In practice, however, the usable workspace of the RP-5AH model is much smaller due to mechanical interferences. Indeed, the robot manufacturer specifies a 297 mm × 210 mm rectangular workspace.

In theory, the design with the largest singularity-free workspace would be one in which all four links are of the same dimension, $l_1 = l_2 = l$, and the motor axes coincide, $d = 0$. The theoretical workspace of such a five-bar robot would be a disc of radius $2l$, the Type 2 singularities of which would be at the disc boundary and at the disc center. However, even if such a robot could be built in practice (and it can't), its usable workspace would be an annulus (i.e., a disc with a hole). This might be useful for some applications, but most applications require continuous rectangular workspaces. Therefore, for comparison purposes, we will assume that the optimal design of a practical five-bar robot that does not switch working modes is the one shown in Fig. 2b.

Our first objective is to show that a practical five-bar robot with link lengths similar to those of the RP-5AH robot, and where switching working modes is possible, could have a larger rectangular workspace than the RP-5AH robot.

Clearly, if the proximal and distal links of a five-bar robot are of different lengths, as in the RP-5AH design the robot's workspace will have holes in it. Then, in order to eliminate this problem, all links should be of the same length, $l_1 = l_2 = l$.

Thus, to find the optimal design, we must determine the offset $d$ with respect to the links' length $l$. Clearly, the smaller the offset, the larger the workspace becomes. However, if $d < l$, then it would not be possible for a proximal link to pass between the two motors due to mechanical interferences. Therefore, $d$ should be just slightly greater than $l$.

The next section will discuss the mechanical design of DexTAR and constitutes the main contribution of this paper. The end-effector can operate directly beneath either motor. Therefore, our optimal design will be one in which the offset $d$ is slightly larger than the length of the links, $l$, and will avoid as many mechanical interferences as possible.

## 3. MECHANICAL DESIGN OF DEXTAR

For demonstration purposes, DexTAR is to pick and place steel balls of 8 mm in diameter. We therefore selected a suction cup for the end-effector and a miniature pneumatic actuator (AEVC from Festo) for its vertical displacement (with a stroke of 10 mm). Since the robot arms should be allowed to rotate freely one over the other, the use of pneumatic tubing (one for the actuator and the other for the suction cup) becomes an important issue. We could not attach the tubes externally because they would get entangled. Therefore, the air should pass through four of the joints.

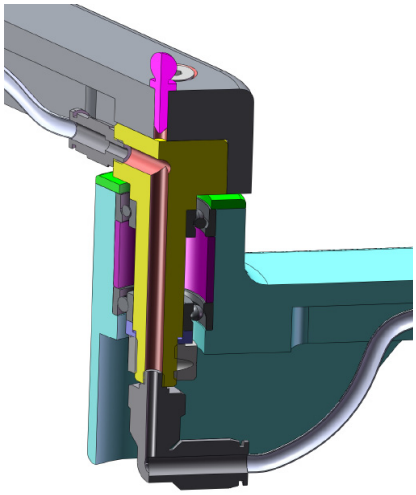

**Fig. 3.** Section view of a passive joint showing the air passage.

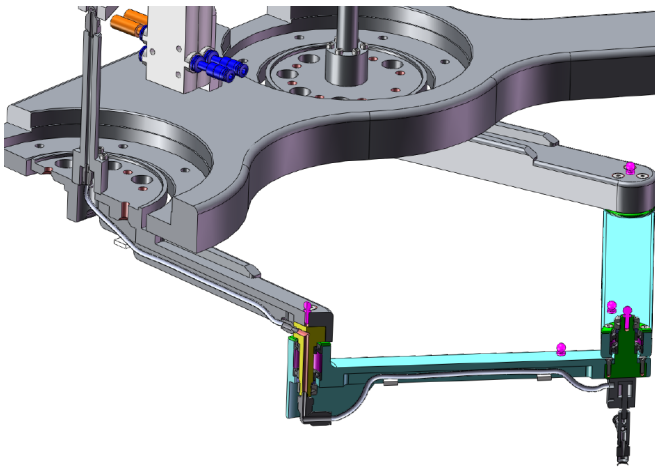

**Fig. 4.** Section view showing the air passage in one of the arms.

For the design of the passive joints we used high precision angular contact ball bearings (7901 CTYNDULP4 from NSK) and spacers. This configuration delivers high level of stability and minimal backlash for the assembly. Figure 3 shows one of the two passive joints that require internal air passage.

The need for internal tubing (Fig. 4) played a decisive role in the motor selection too since we needed to use a motor with a hollow shaft. Fortunately, we already aimed at using direct-drive motors and those are often built with hollow shafts. We set our choice at the Kollmorgen GOLDLINE® rotary motor series.

In order to be able to compare our design to the one of the RP-5AH robot, we selected $l = 230$ mm, so that the sum of the lengths of all links is the same in both designs (920 mm). Then, in order to determine $d$, we summed the values of $l$, the width of the proximal links (38 mm), and a safety gap of 7 mm, which led to the offset $d = 275$ mm.

Our robot should able to fully rotate the proximal and distal links without interferences. Thus, the distal links were designed to be completely below the proximal links and allow considerable overlapping, i.e., the angle between them can be as little as 15° (Fig. 5).

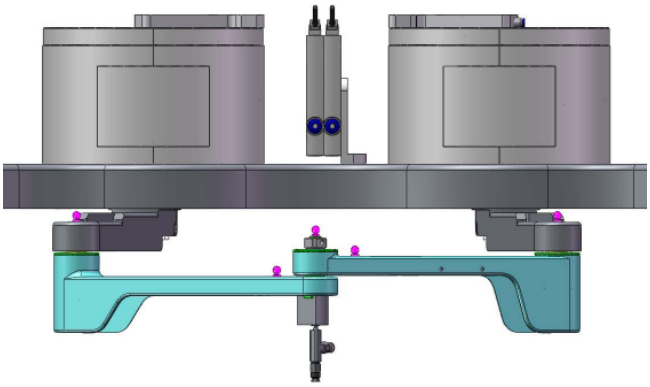

**Fig. 5.** Frontal view of the DexTAR showing some of the measures taken to reduce mechanical interferences.

The final mechanical design of DexTAR is shown in Fig. 6. The small spheres attached at the links (in magenta) are tooling balls that can be used for calibration by a CMM or a measurement arm (though we eventually acquired a laser tracker and no longer need them). It is important to note that the arms of the robot cannot enter into collision with the four supporting columns (not visible in Fig. 6) on which the base plate stands. In other words, the only possible mechanical interferences are between the proximal links (which could hardly be further reduced) and when the distal links make an angle inferior to approximately 15° (which is too close to a Type 2 singularity anyway).

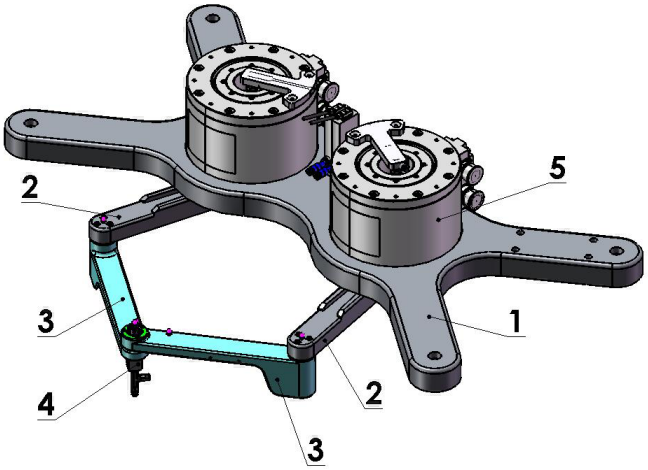


**Fig. 6.** Main components of DexTAR: (1) base plate, (2) proximal links, (3) distal links, (4) end-effector, (5) servo motors.

In addition to reducing mechanical interferences, particular attention was paid to the precision of the robot. We already mentioned the design of the passive joints (Fig. 3) and the choice of direct-drive motors, but we also set a limit to the allowable vertical deflection of the arms, of 50 μm, while keeping the links as light as possible. Using FEM analyses, we optimized the weights of the proximal and distal links at 0.66 kg and 0.37 kg, respectively. We also performed dynamic analyses in order to check for the natural frequencies of DexTAR. The arms are made of aluminum A2024 alloy, while the shafts are made of steel SAE1045.

Then the goal was set to achieve maximum acceleration

of 15 g at the end-effector. In order to determine the required motor torque and acceleration, we performed a number of simulations using the software CosmosWorks. The first step was to establish a trajectory of the end-effector, which we did choosing a straight line of 305 mm to be completed in 0.1 seconds. Using this data we were able to select the servomotor model (Kollmorgen GOLDLINE D063). Among the characteristics of this model we can list zero backlash, low noise level, peak torque of 51 Nm, continuous torque of 17 Nm and an absolute encoder.

Finally, we used a 600 mm × 600 mm breadboard from Thorlabs mounted on three micro-adjustable pads, to hold the steel balls to be manipulated by the robot. The final prototype is shown in Fig. 7. The robot is mounted on a custom-made steel table and is, of course, covered by a safety enclosure (not shown), when in operation.

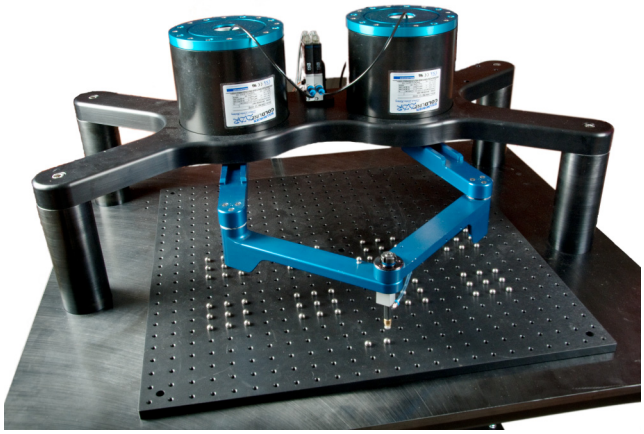

**Fig. 7.** Photo of the DexTAR prototype.

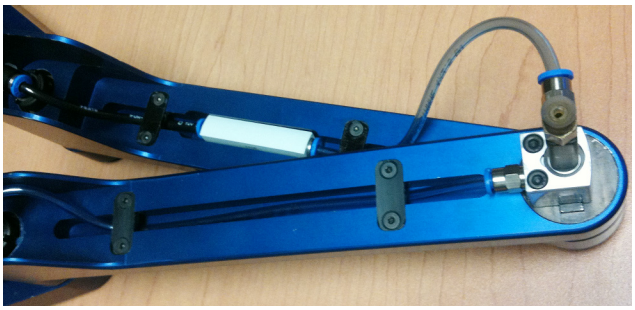

**Fig. 8.** Photo of the distal links in interference.

## 4. ACTIVE JOINT-SPACE AND CARTESIAN WORKSPACE

As explained in [10], the five-bar planar robot has four working modes, each of them representing one solution to the inverse kinematic problem. To switch between these working modes the robot must pass through Type 1 singularities. In this section, we discuss the active joint-space and the Cartesian workspace of the actual DexTAR prototype, rather than the theoretical one, as done in [10].

Figures 9 and 10 show the four working modes and the active joint space for the theoretical design [10]. However these theoretical results do not take into account the mechanical interferences of the real robot.

For the DexTAR prototype, there are only two cases of possible mechanical interferences, as already mentioned. The first one is the interference between the two proximal links. The second one is a limitation in terms of relative angle between the two distal links caused by the passage of the pneumatic tube to the vacuum cup (Fig. 8).

In order to find all mechanical interferences, a discretization in the active-joint space was performed. For each possible combination of $\theta_1$ and $\theta_2$, we calculated the distance between the line segments $O_1A_1$ and $O_2A_2$ (see Figs. 1 and 11). Since the width of the arms is 38 mm and we assumed a safety gap of 2 mm, the distance between the segments $O_1A_1$ and $O_2A_2$ must at least 40 mm to assure that there is no interference between the proximal arms. Furthermore, the angle $A_2CA_1$ should be greater than 15° (Fig. 8).

The resulting active-joint space of the actual DexTAR prototype is shown in Fig. 12. The zone corresponding to mechanical interferences is drawn in black. Thus, the attainable active-joint space is the one in four light colors (i.e., excluding the black area and the white area enclosed by the Type 2 singularity curve in red).

Though it is the active-joint space that will be used for trajectory planning and control of the robot, in this paper, we are mainly interested in the set of positions attainable by our DexTAR prototype from a given home configuration (for example, the one shown in Fig. 7). Indeed, in theory, the only unattainable portion would be the tiny white stripe at the bottom of Fig. 9(b). How big is this portion in DexTAR?

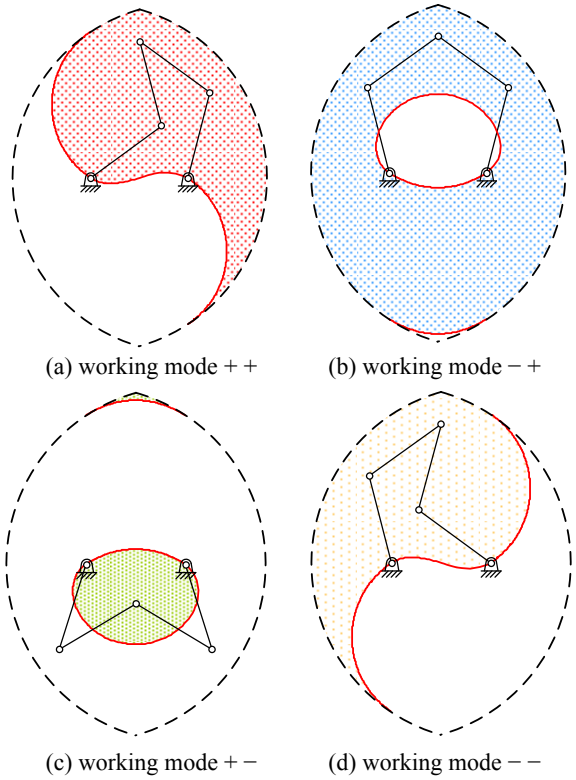

(a) working mode + + (b) working mode − +

(c) working mode + − (d) working mode − −

**Fig. 9.** Singularity-free zones accessible in the first assembly mode for each of the four working modes of DexTAR, disregarding mechanical interferences.

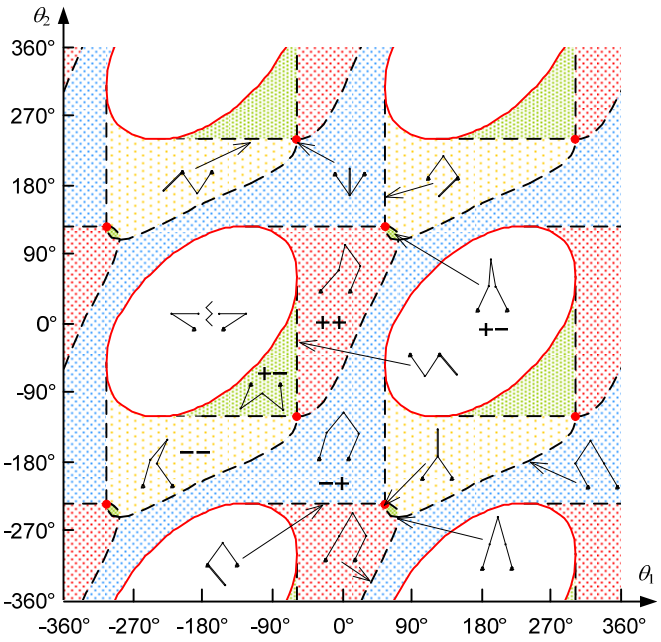


**Fig. 10.** Active-joint space for the first assembly mode of DexTAR showing the Type 2 singularity curves (in red solid line) and points (in red) and the Type 1 singularity curves (in black dashed line), disregarding mechanical interferences.

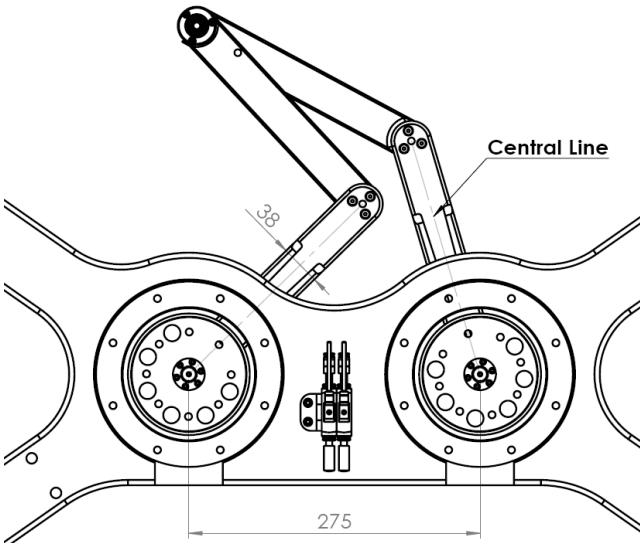


**Fig. 11.** Central lines of the proximal links are used in determining the positions with mechanical interference.

To find the attainable workspace of DexTAR, we basically need to map each of the four colored zones of Fig. 12 onto the Cartesian space, using the direct kinematics, and then obtain their union. In fact, this is done at the same time the active-joint space is obtained. Figure 13 shows the attainable workspace of DexTAR in each working mode. The union of these four areas, shown in Fig. 14, is the workspace of DexTAR, and constitutes the main result of this paper.

It is obvious from Fig. 14 that DexTAR can cover any point within a 400 mm × 400 mm area. Even the best mechanical design of the robot shown in Fig. 2(b) could not cover an area larger than 300 mm × 300 mm. Therefore, our approach leads to a gain of more than 30 % in workspace.

Finally, a Matlab simulation program with an interactive user interface is available at the following address: http://www.parallemic.org/Software/DexTAR.zip. The program allows the user to displace DexTAR in both the Cartesian space and the active-joint space.

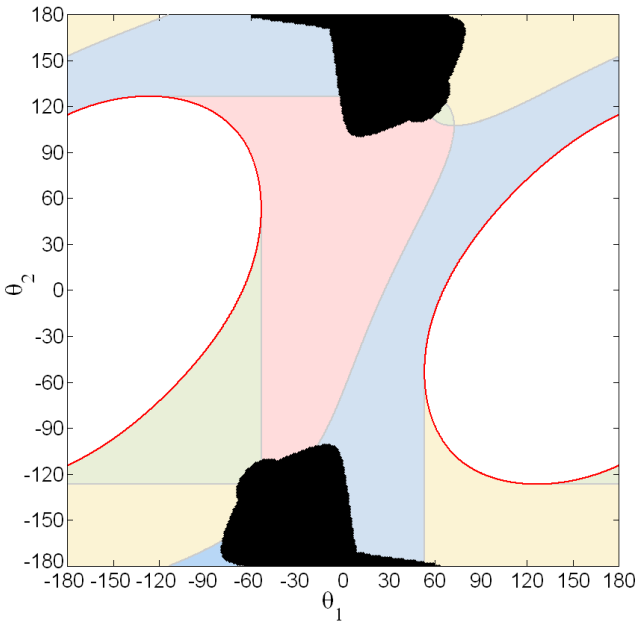


**Fig. 12.** Active-joint space of the DexTAR prototype: Type 2 singularity curves (in red), Type 1 singularity curves (in gray), and mechanical interference zone (in black).

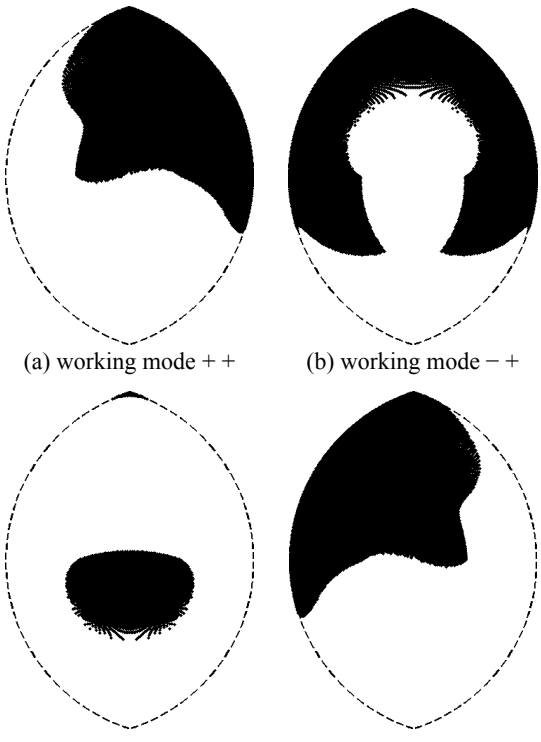

(a) working mode + +  (b) working mode − +

(c) working mode + −  (d) working mode − −

**Fig. 13.** Sets of positions attainable by the DexTAR prototype in the first assembly mode for each of the four working modes.

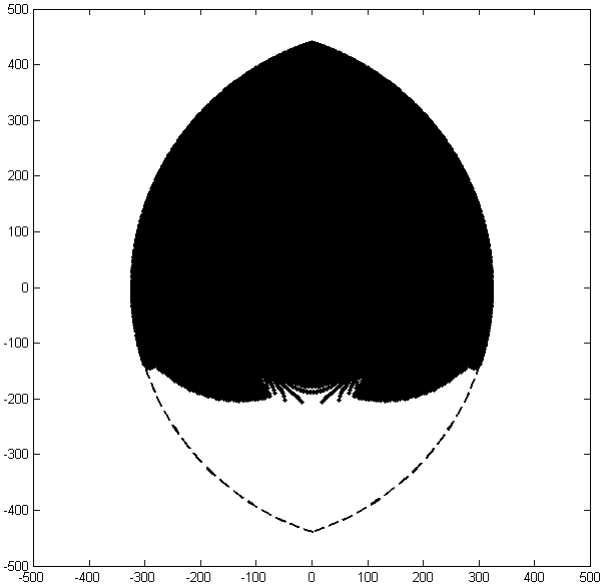


**Fig. 14.** The attainable workspace of DexTAR.

## 5. TRAJECTORY PLANNING

Although trajectory planning will be the subject of another work, we will only briefly recall the main ideas. Let the robot be in a given starting configuration (i.e., point in the active-joint space of Fig. 12). Then, let a desired final position that belongs to the attainable workspace shown in Fig. 14 be given. There are generally four different configurations associated with this final position in the active-joint space shown in Fig. 12. Each configuration corresponds to a different working mode. Therefore, the basic idea is to choose one of the four final configurations based on a mixed set of criteria (proximity to a singularity, time to reach the configuration, etc.). Once a configuration is chosen, the next step will be to apply minimum-time trajectory planning to find the path that minimizes the time to reach this final configuration.

## 6. CONCLUSION

While the approach of crossing Type 1 singularities in order to increase the attainable workspace of some parallel robots is not new, this is the first paper that clearly demonstrates the advantages of this approach in a practical context. Namely, a five-bar parallel robot dubbed DexTAR has been manufactured for that purpose and it was shown that its attainable workspace is at least one third larger than that of a similarly sized five-bar parallel robot that does not cross Type 1 singularities.

## REFERENCES

[1] M. Arsenault and R. Bourdeau, "The synthesis of three-degree-of-freedom planar parallel mechanisms with revolute joints (3-RRR) for an optimal singularity-free workspace," *Journal of Robotic Systems*, Vol. 21, No. 5, pp. 259–274, 2004.

[2] S. Sen, B. Dasgupta and A.K. Mallik., "Variational approach for singularity-path planning of parallel manipulators," *Mechanism and Machine Theory*, Vol. 38, No. 11, pp. 1165–1183, 2003.

[3] A.K. Dash, I-M. Chen, S.H. Yeo and G. Yang, "Workspace generation and planning singularity-free path for parallel manipulators," *Mechanism and Machine Theory*, Vol. 40, No. 7, pp. 778–805, 2005.

[4] X.-J. Liu, J. Wang and G. Pritschow, "Performance atlases and optimum design of planar 5R symmetrical parallel mechanisms," *Mechanism and Machine Theory*, Vol. 41, No. 2, pp. 119–144, 2005.

[5] S. Kock and W. Schumacher, "A parallel x-y manipulator with actuation redundancy for high-speed and active-stiffness applications," *Proceedings of the 1998 IEEE International Conference on Robotics & Automation*, pp. 2295–2300, Leuven, Belgium, May, 1998.

[6] T. Yasuda, D.N. Nenchev., K. Aida and E. Tamuea, "Experiments with a parallel robot with singularity perturbed design," *Proceedings of the 26th Annual Conference of the IEEE Industrial Electronics Society*, Vol. 1, pp. 217–222, 2000.

[7] J. Hesselbach, M. Helm, and S. Soetebier, "Connecting assembly modes for workspace enlargement," *Advances in Robot Kinematics*, J. Lenarcic and F. Thomas (eds.), Kluwer Academic Publishers, The Netherlands, pp. 347–356, 2005.

[8] D. Chablat and P. Wenger, "Regions of feasible point-to-point trajectories in the Cartesian workspace of fully-parallel manipulators," *Proceedings of the ASME Design Technical Conferences*, Paper No. DETC99/DAC-8645, Las Vegas, NV, USA, September 12–15, 1999.

[9] I.A. Bonev and C.M. Gosselin, "Singularity loci of planar parallel manipulators with revolute joints," *Proceedings of the 2nd Workshop on Computational Kinematics*, Seoul, South Korea, pp. 291–299, May 20–22, 2001.

[10] A. Figielski, I.A. Bonev, and P. Bigras, "Towards development of a 2-DOF planar parallel robot with optimal workspace use," *IEEE International Conference on Systems, Man, and Cybernetics*, Montreal, QC, Canada, October 7–10, 2007.